Measurement system design for maximizing the expected utility of monitoring actions

Romain Pasquier[a,*], James-A. Goulet[b], Ian F. C. Smith[a]

[a]*Applied Computing and Mechanics Laboratory (IMAC), School of Architecture, Civil and Environmental Engineering (ENAC), Swiss Federal Institute of Technology (EPFL), CH-1015 Lausanne, Switzerland*
[b]*Department of Civil and Geologic and Mining Engineering, Polytechnique Montréal, Montréal, H3T 1J4, Canada*

Abstract

With the democratization of structural health monitoring and the more and more limited investments dedicated to the infrastructure asset management, efficient monitoring actions are necessary to help owners prioritize the management of infrastructure parks. Efficient monitoring actions include the selection of judicious sensor type and locations and load configurations, in the context of static load tests, in order to optimize the information provided by monitoring interventions and thus, optimize the performance of data interpretation. However, in the context of model-based system identification, approaches that are able to provide direct guidance on whether or not monitor a structure are required based on the their intended utility. This paper proposes an optimization strategy using utility theory and probabilistic behavior prognoses based on model falsification to support decisions related to monitoring interventions. This approach, illustrated by the full-scale case study of a bridge, allows the quantification of the expected utility of measurement systems while indicating the profitability of monitoring actions and is able to determine when monitoring configurations may be reduced by over-instrumentation.

Keywords: Sensor placement, model falsification, utility function, optimization, fatigue assessment, actualized reparation cost.

1. Introduction

With the aging of infrastructure and the limited investments allocated to the structural health management, an increasing number of existing structures are measured. In this context, efficient strategies are required to evaluate the performance of measurement systems prior to site measurements. Such information helps owners prioritize monitoring actions. In order to avoid over-instrumentation and improve performance of the data interpretation, measurement-system design, also called sensor placement, may support the selection of good combinations of sensor types and locations.

---

*Corresponding author. Address: EPFL ENAC IIC IMAC, Station 18, CH-1015 Lausanne, Switzerland. Phone number: +41 21 693 2498
Email address: `rpasquie@gmail.com` (Romain Pasquier)

Model-based data-interpretation techniques are often combined with sensor-placement optimization in order to design the optimal measurement system. Several contributions in this field have based the search for optimal sensor placement on information theory in the purpose of improving parameter estimation. Some authors have maximized either the determinant or the Fisher information matrix to obtain the optimal sensor configuration [10, 24]. Other studied entropy-based approaches [12, 16, 17, 25]. Information entropy depends on the determinant of the Fisher information matrix and both criteria quantify the information associated with model parameters. Stephan [27] mentioned that maximizing some norm of the Fisher information matrix only does not account for potential redundancy of information between selected sensor positions. In addition, although entropy-based approaches have shown to be powerful to optimize measurement systems for improving model predictions, few studies have included systematic modeling uncertainties.

Papadimitriou and Lombaert [18] included the effect of spatially correlated prediction errors in an entropy-based measurement-system-design methodology. They have shown that the minimum distance between sensors is governed by the spatial correlation length of the prediction errors and thus, by accounting for it, redundancy of information is avoided. In addition, assumptions of uncorrelated prediction errors in models may lead to sub-optimal measurement systems.

Papadopoulou et al. [19] underlined limitations associated with potential redundancy of information using individual-sensor entropy metric and proposed a methodology that maximizes the joint entropy between sensor locations. This study has shown that the joint-entropy design criterion is able to improve model predictions at unmeasured locations compared with common entropy maximization.

Several researches have concentrated on optimization algorithms to determine optimal configurations [11, 28–30]. One of the most widely used algorithm is the genetic algorithm. However, many authors have preferred sequential algorithms to global search algorithms that are computationally demanding [7, 15, 18, 19]. Sequential algorithms such as forward and backward sequential algorithm are part of the family of heuristic optimization. Their search for near optimal solutions often led to good approximations of the optimal measurement-system configuration [18].

Methodologies mentioned above focus on the sensor information accuracy to design measurement systems. As emphasized by Pozzi and Der Kiureghian [22], the value of information should reside in its potential to guide decisions. As a result, measurement systems should be designed for their intended utility. However, few methodologies have quantified the value of information provided by measurement systems, except some authors who evaluated the economic value of the information acquired by on-site sensors [23, 32].

Recognizing this aspect, Goulet and Smith [7] proposed a methodology where the usefulness of a measurement system is quantified though the metric of expected identifiability. This approach is able to quantify over-instrumentation. Indeed, Goulet and Smith [7] demonstrated that over-instrumentation appears when the new information provided by additional measurements is exceeded by the amount of uncertainty provided by the inclusion of new measurements. In addition, this methodology includes systematic modeling uncer-

tainties induced by simplifications and omissions in the model-class building and determines good trade-offs between interpretation goals and available economic resources. However, this measurement-system-design methodology is limited to the expected performance of the behavior diagnosis.

In the context of model-based data interpretation, the optimal solution is usually related to the way structural-behavior diagnosis and prognosis are evaluated. In addition, most of the existing measurement-system-design strategies are based on the minimization of the model-parameter uncertainty at the diagnosis stage. However, reducing the uncertainty in remaining-life prognosis of structural components is often more relevant since remaining-life prognosis is able to directly support decisions related to repair.

This paper proposes a novel strategy for sensor placement that is based on the expected utility of measurement systems. Physics-based-model parameters are identified using error-domain model falsification, a data-interpretation technique that accommodates populations of model instances [9]. A population-based prognosis methodology is then used to predict the remaining life of structural components [20, 21]. Then, this prognosis is used to derive the reparation costs including monitoring costs, and further the expected utility of measurement systems. This strategy uses a greedy algorithm to evaluate a near-optimal solution of the sensor-placement problem. This measurement-system-design strategy described in this paper determines optimal measurement systems in terms of expected utility, and this includes economic aspects. This approach is able to evaluate whether or not monitoring actions are profitable and when measurement-system performance becomes reduced by overinstrumentation.

1.1. Utility functions

In the field of decision theory, a rational approach to choose between alternative actions when the consequences of such choices are not known is the use of utility theory and probability theory. When making decision under risk, the possible outcomes may be evaluated through an utility and a probability of occurrence. As a result, *"the decision maker [...] cannot guarantee that the outcome will be as good as he might hope for, but he has made the best decision he can, based on his preferences and available knowledge"* [14].

A convenient manner to describe preferences is the *utility function*. Utility functions provide a ranking to alternatives of a choice set. They describe the risk attitude of the decision maker. Three types of risk attitudes are defined: (1) risk averse, (2) risk neutral, and (3) risk loving. A risk-averse person has a preference for an income that is certain over an uncertain income with larger expected value. For this reason, risk-averse utility function are monotone and quasi-concave as shown in Figure 1.

Under uncertainty, for the same income, a risk-averse person finds this outcome to be better than a risk-neutral person. In addition, if $A = 0\,\$$ and $B = 1\,\$$, the relative utility $\mathbb{U}(B) - \mathbb{U}(A)$ will be much higher than if $A' = 100\,\$$ and $B' = 101\,\$$ in the case of a risk-averse behavior. This intuitively reflects the common human behavior which will be indifferent to receive either $100\,\$$ or $101\,\$$.
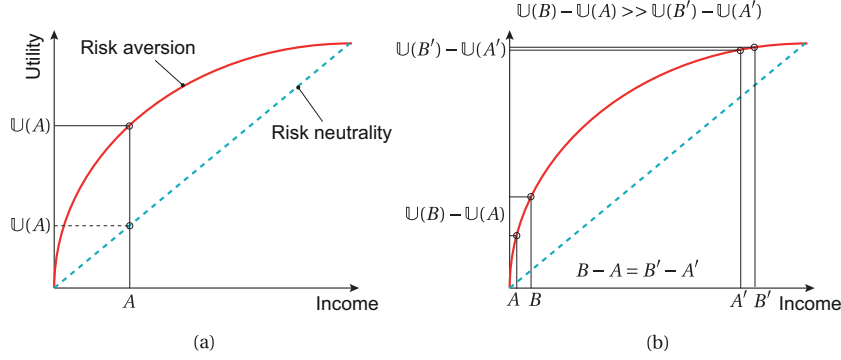
Figure 1: Schematic comparison of risk-averse function and risk-neutral function. (a) Under uncertainty, for an equivalent income, a risk-averse person finds more useful this income than a risk-neutral person. (b) For $A = 0\,\$$ and $B = 1\,\$$, the relative utility $\mathbb{U}(B) - \mathbb{U}(A)$ will be much higher than if $A' = 100\,\$$ and $B' = 101\,\$$ in the case of a risk-averse behavior.

In the management of risky situations, where decisions are made under uncertainty, the *expected utility* is usually assessed. The first expected utility model was proposed by Cramer and Bernoulli during the 18th century [13] and solved by Daniel Bernoulli [2]. The latter argued for a logarithmic utility function, which matches with human behavior for risk aversion.

Expected utility functions are commonly used in economics and finance to model human behavior in relation with money. For this reason, utility functions often describe the relationship between money and expected utility. Utility functions have also been used to assess the engineering performance in construction projects [6], for structural inspection planning [5] and risk assessment of structural failure [3]. However, for measurement-system design, utility functions have not yet been applied to quantify the expected utility of monitoring actions.

Section 2 presents the measurement-system-design methodology combining utility theory and behavior prognosis (Section 2.2). The methodology is illustrated for the case of remaining-fatigue-life prognosis of critical connections. The optimization strategy is then presented in Section 2.3. Finally, an application of this methodology to the reparation of critical connections of a full-scale case study is then presented in Section 3.

2. Methodology

This methodology combines model falsification and utility theory for optimizing measurement systems in order to maximize the utility of monitoring actions based on remaining-fatigue-life estimations of structures.

Along the text, standard variables and indexes are denoted by lower-case letters, e.g. "x". Random variables are denoted by upper-case letters, "X", and realizations of random variables are denoted by "$\tilde{x}$". Estimations are denoted by a hat symbol, i.e. "$\hat{x}$" and mean values by an over-line symbol, i.e. "$\overline{x}$". Vectors, matrices and sets are represented by bold characters, i.e. "$\mathbf{x}, \tilde{\mathbf{x}}$, or $\mathbf{X}$". Matrices and vectors are defined between square brackets and sets between braces.

4

In the context of system identification, it is assumed that $\boldsymbol{\Theta} = [\Theta_1, \Theta_2, \cdots, \Theta_{n_\theta}]^\intercal$ is a vector of parameters described by random variables and $\boldsymbol{\Gamma} = [\Gamma_1, \Gamma_2, \cdots, \Gamma_{n_\gamma}]^\intercal$ a vector of random variables used in a model $g(\mathbf{x}, \boldsymbol{\Gamma}, \boldsymbol{\Theta})$ for predicting the structural responses $\mathbf{Y} = [Y_1, Y_2, \cdots, Y_{n_y}]^\intercal$ so that

$$\mathbf{Y} = g(\mathbf{x}_m, \boldsymbol{\Gamma}_m, \boldsymbol{\Theta}) + \mathbf{U}_g \tag{1}$$

where $\mathbf{U} = [U_{g,1}, U_{g,2}, \cdots, U_{g,n_y}]^\intercal$ represents the modeling errors and the indicator matrix $\mathbf{x}_m$ describes each of the n_y degrees of freedom where the structural response is measured.

In addition, observations of the structural responses $\hat{\mathbf{y}}$ defined by

$$\mathbf{Y} = \hat{\mathbf{y}} + \mathbf{U}_{\hat{y}} \tag{2}$$

are used to improve our knowledge of model parameters $\boldsymbol{\Theta}$. This procedure is described in Section 2.1. The improved estimate of $\boldsymbol{\Theta}$, denoted $\boldsymbol{\Theta}''$, is then used to perform prognosis on unobserved quantities Z'' defined so that

$$Z'' = h\big(g(\mathbf{x}_p, \boldsymbol{\Gamma}_p, \boldsymbol{\Theta}'') + U_g\big)\big) + U_h \tag{3}$$

where the function $h(\cdot)$ consists in a post-processing of predicted structural responses, where U_h is a random variable describing the post-processing error. For example, this prognosis may be remaining-fatigue-life estimations and prediction of the reparation cost of critical connections. The latter behavior prognosis procedure is presented in Section 2.2.

Finally, the goal of this methodology is to provide a framework for optimizing measurement systems, $\mathbf{x}_m$ so that the *expected utility* of the unobserved quantities Z'' is maximized,

$$\mathbf{x}_m^* = \arg\max_{\mathbf{x}_m} \mathbb{E}[\mathbb{U}(Z'')] \tag{4}$$

The utility function $\mathbb{U}(\cdot)$ and the expected utility maximization framework are described in Section 2.3. Practical application of the methodology proposed here will often lead in problems that are analytically intractable. Section 2.3.1 presents the formulation of a Monte Carlo estimation method for computing the expectation $\mathbb{E}[\cdot]$ presented in Eq. (4) and Section 2.3.2 describes a greedy algorithm based on sequential optimization to approximate the optimal solution.

2.1. Model falsification

The model falsification procedure used here was proposed by Goulet and Smith [9]. This procedure consists in falsifying all model instances that are instantiations of parameter-value combination for which the resulting model prediction are not compatible with measurement data given modeling and measurement

uncertainties. The set of candidate models obtained after falsification is defined by

$$\mathbf{\Omega}'' = \left\{ \boldsymbol{\theta} \in \mathbf{\Omega} \middle| \; \forall i : \Pr(u_{i,\text{low}} \leq r_i \leq u_{i,\text{high}}) \leq \phi^{1/n_y} = \int_{u_{i,\text{low}}}^{u_{i,\text{high}}} f_{U_i}(u_i) \, \mathrm{d}u_i \right\} \tag{5}$$

where the residuals r_i are defined so that

$$\mathbf{r} = [r_1, r_2, \cdots, r_{n_y}]^{\mathsf{T}} = g(\mathbf{x}_m, \overline{\boldsymbol{\gamma}}_m, \boldsymbol{\theta}) - \hat{\mathbf{y}} \tag{6}$$

The combined uncertainties $\mathbf{U}$ are defined by

$$\mathbf{U} = [U_1, U_2, \cdots, U_{n_y}]^{\mathsf{T}} = \mathbf{U}_{\hat{y}} - \left(g(\mathbf{x}_m, \mathbf{\Gamma}_m, \overline{\boldsymbol{\theta}}) - g(\mathbf{x}_m, \overline{\boldsymbol{\gamma}}_m, \overline{\boldsymbol{\theta}}) + \mathbf{U}_g \right) \tag{7}$$

and ϕ denotes the target reliability. All model instances that have been falsified are assigned a probability of 0 so that

$$\Pr(\mathbf{\Theta} = \theta \notin \mathbf{\Omega}'') = 0 \tag{8}$$

and all parameter values not belonging to the falsified set, $\boldsymbol{\theta} \in \mathbf{\Omega}''$, are labeled as *candidate models* and are assigned a constant probability

$$\Pr(\mathbf{\Theta} = \boldsymbol{\theta} \in \mathbf{\Omega}'') = \frac{1}{\int_{\boldsymbol{\theta} \in \mathbf{\Omega}''} d\boldsymbol{\theta}} \tag{9}$$

Consequently, $\mathbf{\Theta}''$ is defined as the vector of random variables describing the candidate parameter values of $\boldsymbol{\theta}$ given measurement data, $\hat{\mathbf{y}}$. Its probability density function is

$$f_{\mathbf{\Theta}''}(\boldsymbol{\theta}) = \begin{cases} \frac{1}{\int_{\boldsymbol{\theta} \in \mathbf{\Omega}''} d\boldsymbol{\theta}}, & \text{if } \boldsymbol{\theta} \in \mathbf{\Omega}'' \\ 0, & \text{otherwise} \end{cases} \tag{10}$$

2.2. Behavior prognosis

Any structural-behavior prognosis of interest may be used to determine the utility of monitoring actions. In this paper, it is proposed to illustrate the methodology through remaining-fatigue-life estimations, presented in Section 2.2.1 and evaluating the expected utility of monitoring actions through cost considerations in Section 2.2.2.

2.2.1. Application to bridge remaining-fatigue-life prognosis

A prognosis of interest may be the remaining-fatigue-life estimation of bridge critical connections as proposed in [21]. For the prediction of remaining fatigue life, a number of cycles under constant stress-range level can be used. This approach that is described in common construction codes [1, 4, 26] uses a single traffic-axle loading and constant stress amplitudes to determine the remaining number of cycles to failure.

6

Constant stress-ranges are determined by calculating the maximum and minimum stresses resulting from the influence line of the moving traffic-axle loading. The stress-range value is defined by $\Delta\sigma = \sigma_{\max} - \sigma_{\min}$, where σ is the stress induced in the critical connection by the axle loading. The relation between the stress-range and the number of cycles to failure n_f is given by $n_f = a \cdot \Delta\sigma^{-b}$, where a is a constant depending on the detail category and b is a measure of the fatigue crack-growth rate. S-N curves describing this relation are available in construction codes and design guides [26, 31]. The remaining fatigue life is determined by

$$\mathbf{RFL} = k \cdot \mathbf{\Delta\sigma}^{-b} = k \cdot \left(\left(g(\mathbf{x}_p^{\max}, \mathbf{\Gamma}_p, \mathbf{\Theta}) + \mathbf{U}_g^{\max} \right) - \left(g(\mathbf{x}_p^{\min}, \mathbf{\Gamma}_p, \mathbf{\Theta}) + \mathbf{U}_g^{\min} \right) \right)^{-b} \tag{11}$$

where $k = \frac{70}{2 \cdot 10^6} \cdot a$ in order to account for the damage equivalence factor that compensates for the simplified traffic-load model [26]. This factor is calibrated to verify the fatigue resistance for $2 \cdot 10^6$ load cycles and a service life of 70 years. Such correction has to be done in order to evaluate the effective damage in the connection. In addition, in Eq. (11), $\mathbf{x}_p^{\max}$ and $\mathbf{x}_p^{\min}$ represents the indicator matrix of the maximum and minimum stresses resulting from the influence line. The modeling uncertainty $\mathbf{U}_g^{\max}$ and $\mathbf{U}_g^{\min}$ associated with the maximum and minimum stress predictions originates from the same sources that are determined during the model-falsification task and is evaluated for the critical locations studied.

This simplified approach is used to evaluate the remaining fatigue life of connections because few computing resources are required. Furthermore, this approach returns conservative remaining-life predictions.

2.2.2. Prognosis of reparation cost based on fatigue assessment

Measurement-system optimization based on direct fatigue assessment would involve $\mathbf{Z}'' = \mathbf{RFL}'' = [RFL_1'', \ldots, RFL_{n_p}'']^\intercal$ and lead to the separate maximization of remaining fatigue life of each critical connection. For large numbers of connections, such approaches may lead to difficulty in interpreting the utility of monitoring and to unprofitable interventions.

Engineers are rather interested in the benefit of performing a monitoring task in comparison with the cost of reparation. By improving the remaining-fatigue-life estimations using an optimal measurement system, it is possible to evaluate beforehand if the cost of the monitoring task will be worth postponing the repair.

Let c_r be the cost of repairing a single connection. This operation is considered effective at the end of the connection fatigue life. The absolute *present value* of this investment is less than its value in the future assuming positive discount rates. The principle of present value is widely used in finance to determine the value of an expected income that occurs at a future date. Usually, the present value is defined by

$$pv = \frac{c_r}{(1+i)^t} \tag{12}$$

where t is the number of years between the present date and the date where the cost is worth c_r and $i > 0$ is the discount rate for a year. The discount rate accounts for the uncertainty associated with future value

7

of cash flows is determined by federal reserve banks through market analyses.

When improving the remaining-fatigue-life estimation RFL_j'' of a connection j through structural monitoring, the present value of the reparation cost decreases as t increases. Depending on the cost of the measurement system, it may or not be financially profitable to improve remaining-fatigue-life predictions. The total cost is also related to the number of connections to be evaluated. The total cost Z'' of the monitoring that includes the evaluation of n_p critical connections that would need to be repaired is

$$Z'' = c_m + \sum_{j=1}^{n_p} \frac{c_r}{(1+i)^{RFL_j''}} \tag{13}$$

where c_m is the cost of monitoring including the cost of load tests, measurement instruments and data interpretation. The right side of this equation represents the function $h(\cdot)$ of Eq. (3) and $U_h = 0$. Note that Z'' is a random variable since it depends on the random variable RFL_j.

2.3. Measurement system optimization

The measurement system optimization is necessary to identify which structural responses to measure, $\mathbf{x}_m$, so that the *expected utility* of Z'' is maximized. The expected utility is defined by

$$\mathbb{E}[\mathbb{U}(Z'')] = \int \mathbb{U}(z) f_{Z''}(z) dz \tag{14}$$

where the utility function $\mathbb{U}(z)$ includes the preference related to the values of z. In several practical cases, $\mathbb{U}(z)$ is non-linear and its first derivative has monotonically decreasing values.

A common utility function for describing such a situation is the logarithmic function, $\ln z$, in agreement with Bernoulli's proposal [2]. However, since the goal of the methodology is the maximization of the expected utility and since z is related to the cost of reparation that needs to be minimized, the inverse of the logarithm is preferred:

$$\mathbb{U}(z) = \ln(const - z) \tag{15}$$

With such definition, the utility of a measurement system decreases for increasing total cost z''. Note that this function is undefined for negative values of $const - z$. In order to avoid these values and keep utility calculation unbiased, the constant is chosen to be $const = c_r \cdot n_p$. Although this modifies the utility value, the relative change in utility values between measurement systems is preserved.

2.3.1. Monte Carlo estimation

Since at this stage measured values are unknown, Eq. (2) cannot be satisfied based on on-site measurements $\hat{\mathbf{y}}$ and measurement uncertainty $\mathbf{U}_{\hat{y}}$. Some current proposals employ simulated measurements based

8

on the combination of a random selection of $\boldsymbol{\Theta}$ and a set of modeling and measurement uncertainties that are correlated through qualitative values.

Figure 2 presents distributions of correlation values between uncertainties that refers to the qualitative reasoning used in [7]. Depending on the source of uncertainty, its correlation value of the errors between sensor types and locations may be low, moderate or high in both signs. The user selects the level of correlation and random samples are drawn from the corresponding distribution of values that are used when combining uncertainties.
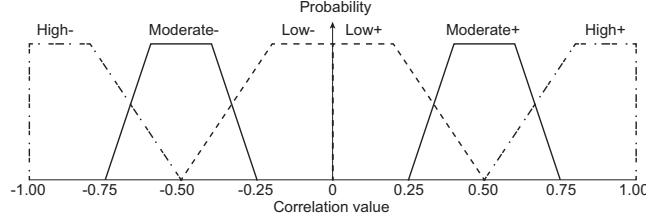

Figure 2: Distribution of correlation values of errors between sensor types and locations within a qualitative reasoning scheme. Users only define qualitatively correlation values between uncertainties by low, moderate, high, negative and positive. Adapted from [8].

For most practical problems, $\mathbb{E}[\mathbb{U}(Z'')]$ cannot be estimated analytically for a given measurement configuration $\mathbf{x}_m$. A generally applicable alternative is to use Monte Carlo simulations to draw first samples of simulated measurements from the initial population of model instances Ω,

$$\tilde{\mathbf{y}}_s = g(\mathbf{x}_m, \tilde{\boldsymbol{\gamma}}_{s,m}, \tilde{\boldsymbol{\theta}}_s) - \tilde{\mathbf{u}}_{s,\rho} \tag{16}$$

where the index ρ indicates that uncertainties are correlated through qualitative reasoning. Simulated measurements lead to identification of a candidate model set Ω''. Then, the expected utility can be approximated by

$$\mathbb{E}[\mathbb{U}(Z'')] \approx \mathbb{E}[\widehat{\mathbb{U}(Z'')}] = \frac{1}{n_s} \sum_{s=1}^{n_s} \mathbb{U}(\tilde{z}''_s) \tag{17}$$

where $\tilde{z}''_s$ is one of the n_s realizations of Z'' obtained by evaluating the function

$$\tilde{z}''_s = h(g(\mathbf{x}_p, \tilde{\boldsymbol{\gamma}}_{s,p}, \tilde{\boldsymbol{\theta}}''_s) + \tilde{\mathbf{u}}_{s,g}) + \tilde{\mathbf{u}}_{s,h} \tag{18}$$

using samples simultaneously obtained for $\{\tilde{\mathbf{y}}_s, \tilde{\boldsymbol{\gamma}}_{s,m}, \tilde{\boldsymbol{\theta}}_s, \tilde{\mathbf{u}}_{s,\rho}, \tilde{\boldsymbol{\gamma}}_{s,p}, \tilde{\boldsymbol{\theta}}''_s, \tilde{\mathbf{u}}_{s,g}, \tilde{\mathbf{u}}_{s,h}\}$.

2.3.2. Measurement-system-optimization strategy

The space of possible sensor combinations and permutations of measurements grows exponentially with the size of $\mathbf{x}_m$. For practical applications, the search space is often discrete and non-convex so that optimiza-

tion algorithms are necessary to approximate the global optimum. In this paper, the measurement-system optimization is performed using a greedy algorithm. A flowchart of the process leading to the maximum expected utility is presented in Figure 3.

This methodology identifies sequentially from an initial sensor configuration $\mathbf{x}_m = [11\ldots1]$ of $n = n_y$ locations which sensor to remove in order to maximize a single objective, the expected utility. The process of sensor removal continues until a single location is left. In situations where static-load tests are optimized, the process terminates when a single load case and a single sensor remain.

Along with the initial sensor configuration, a set of n sensor configurations is generated with all combinations of $n-1$ sensor locations. For each sensor configuration, the expected utility is computed. The expected utility is calculated using n_s draws of simulated measurements referring to the selected sensor configuration. The initial population of model instances is used to randomly select a set of parameters $\boldsymbol{\theta}_s$. Then, candidate-model sets are determined by falsifying model instances of the initial population that are not compatible with simulated measurements.

Once the expected value of each sensor configuration containing $n-1$ sensors is computed and stored, the algorithm searches for the configurations of $n-1$ sensors that maximize the expected utility. This configuration refers to the removal of sensor location k. Since the location k refers to sensor removal among n sensors that lead to the best performance, it is meaningful that the algorithm continues the search for the best expected utility without this sensor location. Although this sensor is permanently removed, the sensor configuration is stored for building the curve of maximum solutions at the end of the process.

Thus, the process continues with $n = n-1$ sensors. This process is repeated successively until a single sensor remains. Then, the cost of each sensor configuration that has been computed to determine the expected utility is used to remove solutions that are dominated by a better utility. In this way, the optimal expected utility can be paired with its number of measurements including the number of load configurations in order to select the optimal measurement system. This algorithm relies on a backward sequential strategy. However, in order to increase the chances of finding the global optimum $\mathbf{x}_m^*$, a forward sequential (increasing number of sensors) strategy is used with the starting configuration being the ending configuration of the backward search.

When the optimal solution refers to a sensor configuration and thus, an expected utility that is greater than the utility without the monitoring system, monitoring interventions are profitable. When the optimal solution is found without monitoring necessity, it may be possible to search for other potential measurement locations and types and restart the algorithm. If such measurements are not possible, such results justify forgoing monitoring interventions. In such situations, reparation costs cannot be reduced by improved evaluation of fatigue reserve capacity, and the prognosis is thus made based on the initial population of model instances.

Also, the curve of the maximum expected utility related to the monitoring costs may reveal that
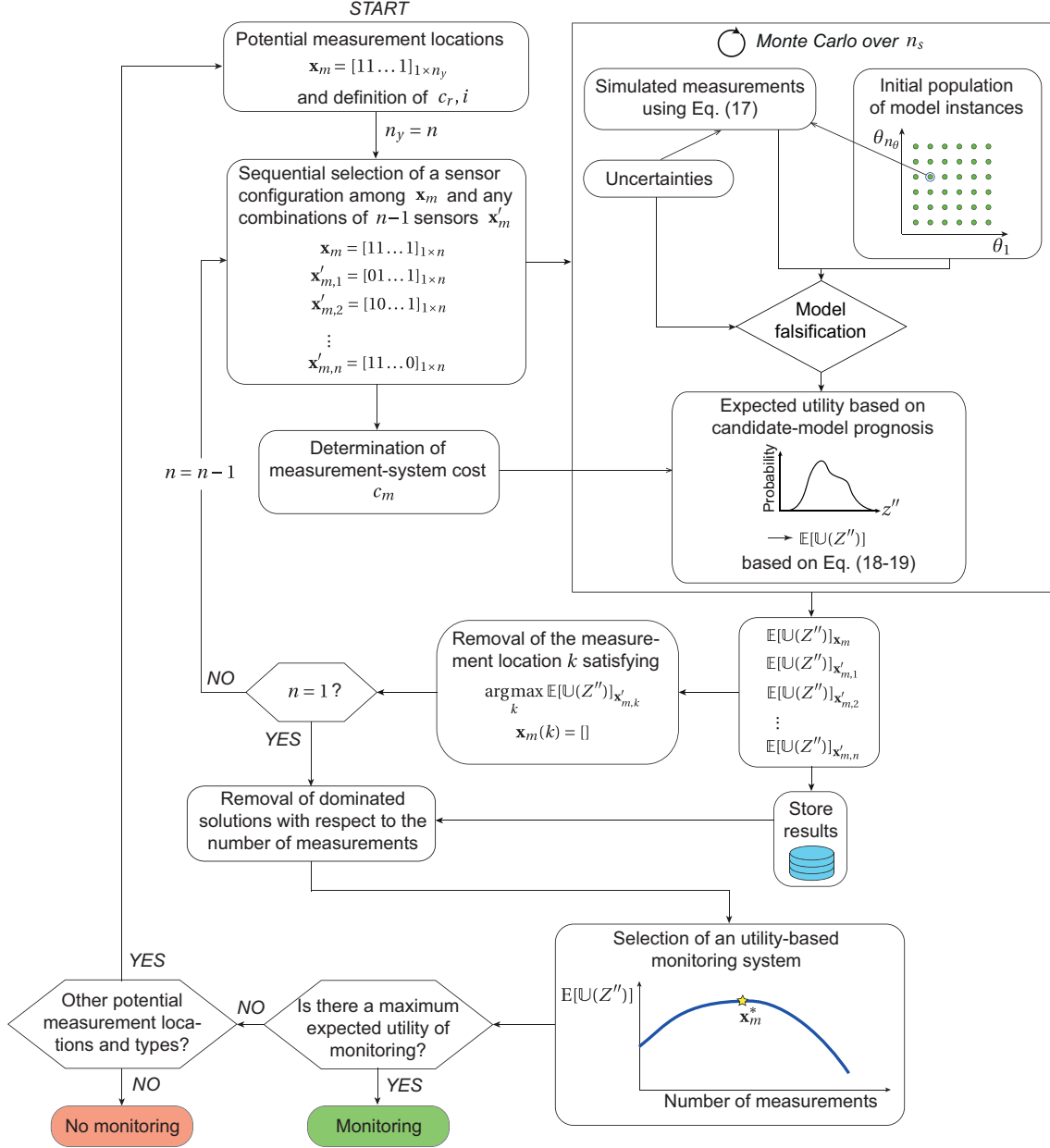
10

START

Potential measurement locations
$\mathbf{x}_m = [11\ldots 1]_{1\times n_y}$
and definition of c_r, i

$n_y = n$

Sequential selection of a sensor
configuration among $\mathbf{x}_m$ and any
combinations of $n-1$ sensors $\mathbf{x}'_m$

$\mathbf{x}_m = [11\ldots 1]_{1\times n}$
$\mathbf{x}'_{m,1} = [01\ldots 1]_{1\times n}$
$\mathbf{x}'_{m,2} = [10\ldots 1]_{1\times n}$
$\vdots$
$\mathbf{x}'_{m,n} = [11\ldots 0]_{1\times n}$

Determination of
measurement-system cost
c_m

Monte Carlo over n_s

Simulated measurements
using Eq. (17)

Initial population
of model instances

θ_{n_θ}

θ_1

Uncertainties

Model
falsification

Expected utility based on
candidate-model prognosis

Probability

z''

$\rightarrow \mathbb{E}[\mathbb{U}(Z'')]$
based on Eq. (18-19)

$\mathbb{E}[\mathbb{U}(Z'')]_{\mathbf{x}_m}$
$\mathbb{E}[\mathbb{U}(Z'')]_{\mathbf{x}'_{m,1}}$
$\mathbb{E}[\mathbb{U}(Z'')]_{\mathbf{x}'_{m,2}}$
$\vdots$
$\mathbb{E}[\mathbb{U}(Z'')]_{\mathbf{x}'_{m,n}}$

Removal of the measure-
ment location k satisfying
$\underset{k}{\arg\max}\,\mathbb{E}[\mathbb{U}(Z'')]_{\mathbf{x}'_{m,k}}$
$\mathbf{x}_m(k) = []$

NO

$n = 1\,?$

YES

$n = n-1$

Removal of dominated
solutions with respect to the
number of measurements

Store
results

Selection of an utility-based
monitoring system

$\mathrm{E}[\mathbb{U}(Z'')]$

$\mathbf{x}_m^*$

Number of measurements

YES

Other potential
measurement loca-
tions and types?

NO

Is there a maximum
expected utility of
monitoring?

YES

NO

No monitoring

Monitoring

Figure 3: Process flowchart of utility-based measurement-system design using greedy algorithm.

11

measurement systems beyond the optimum decrease the performance of utility and thus, indicate over-instrumentation.

3. Case studies

The example that is used to illustrate the measurement-system-design methodology is a composite-steel-concrete bridge located in the city of Aarwangen (Switzerland). The bridge has two spans of $47.8\,\mathrm{m}$ with welded tubular steel trusses connected in a composite manner to the concrete deck that is $8.3\,\mathrm{m}$ wide. A 3D finite-element model is first built based on the bridge drawings (also described in [20, 21]). The cross-section of the finite-element model and its general overview are displayed in Figure 4.
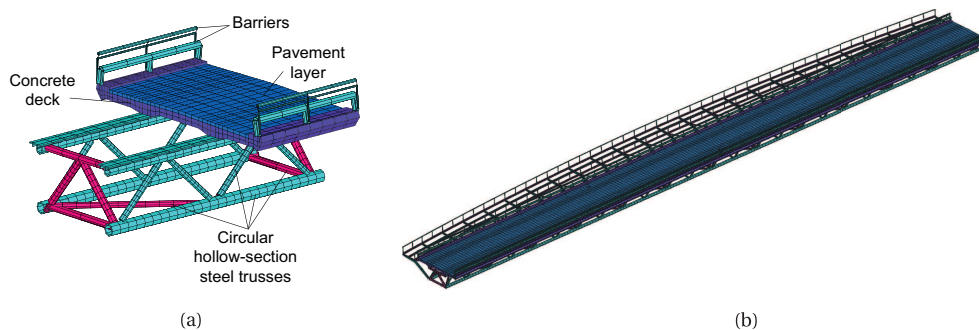

Figure 4: (a) Aarwangen Bridge model cross-section and (b) general overview [ASK PERMISSION Reprinted from Pasquier et al. [21]].

The main assumption that is made includes the simplification of the connection behavior using rotational springs and pinned rigid beams such as illustrated in Figure 5. Also, the connection between the concrete deck and the steel trusses are assumed to be perfect and the bearing devices are simplified by perfect expansion and fixed supports since they were in good condition.
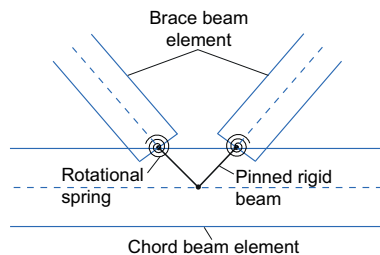

Figure 5: Aarwangen Bridge connection model.

In addition, several characteristics of the structure are unknown and have potentially a significant influence on the structural response: the rotational stiffness of the truss connections (modeled by springs) and the Young's moduli of concrete and pavement. In addition, an in-situ inspection has highlighted a potential

significant effect of the longitudinal stiffness of the pavement covering expansion joints. The model class includes thus these unknown parameters. As illustrated in Figure 6, the rotational stiffness of the truss connections is represented by rotational springs connected between the diagonal members and either the upper or lower chord. Expansion joints are modeled using springs parallel to the bridge longitudinal axis.
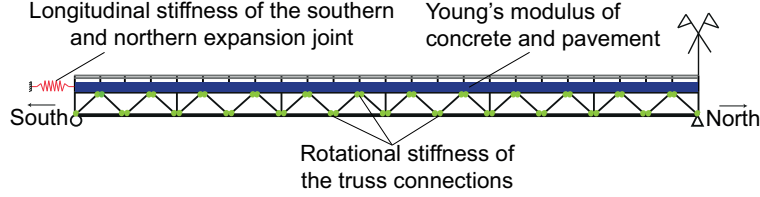

Figure 6: Aarwangen Bridge model parameters. Adapted from [20].

Possible parameter values for spring stiffnesses are sought for both the southern and northern abutments. These structural properties are to be identified using behavior measurements. Other uncertainties, such as steel Young's modulus, concrete Poisson's ratio, truck weight and member dimensions, have a secondary influence on the structural behavior. In Pasquier et al. [20], it has been found that the Young's modulus of steel has a low influence of remaining-fatigue-life predictions.

The goal of this study is the determination of the best measurement system (load-test and sensor configuration) among potential load cases, sensors and sensor locations through maximizing the expected utility of monitoring. The purpose of monitoring actions is the maximization of the expected utility based on reparation cost of the four critical connections displayed in Figure 7.
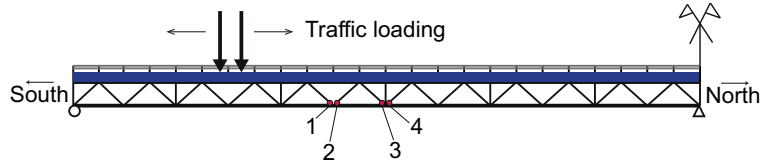

Figure 7: Aarwangen Bridge critical connections and code traffic loading. Adapted from [21].

Initial parameters values $\boldsymbol{\theta} = [\theta_1, \theta_2, \ldots, \theta_5]$ and their initial range of values are presented in Table 1. PDFs of secondary parameter random variables Γ are displayed in Table 2. These PDFs are estimated using engineering heuristics [21].

Note that the variability of profile thickness and diameter $\gamma_{m,4}$ and $\gamma_{m,6}$ of critical connections under study are not taken into account during prognosis of remaining fatigue life since such uncertainties are already included in the S-N curve elaboration.

In order to test the measurement-system-design methodology described in Section 2, four potential load configurations are proposed in Figure 8. Each load case involves four trucks positioned either symmetrically

Table 1: Initial-model parameter ranges for the Aarwangen Bridge

Parameter θ	Units	PDF	Min	Max
Θ_1: Rotational stiffness of truss connections	MNm/rad	Uniform	10^{-1}	10^3
Θ_2: Stiffness of southern expansion joint	MN/m	Uniform	10^{-1}	10^4
Θ_3: Stiffness of northern expansion joint	MN/m	Uniform	10^{-1}	10^4
Θ_4: Young's modulus of concrete	GPa	Uniform	20	50
Θ_5: Young's modulus of pavement	GPa	Uniform	2	20

Table 2: Aarwangen Bridge secondary parameter random variables γ and their PDF as inputed in the Monte Carlo simulation.

Parameters γ_m, γ_p	Description	Unit	PDF	Mean/Min	SD/Max
$\Gamma_{m,1}$, $\Gamma_{p,1}$	Young's modulus of steel	GPa	Gaussian	207	2
$\Gamma_{m,2}$, $\Gamma_{p,2}$	Δv Poisson's ratio of concrete	-	Gaussian	0.19	0.025
$\Gamma_{m,3}$, $\Gamma_{p,3}$	Δt pavement thickness	%	Gaussian	0	2.5
$\Gamma_{m,4}$	Δt_1 steel profile thickness	%	Uniform	-10	10
$\Gamma_{m,5}$, $\Gamma_{p,4}$	Δt_2 steel profile thickness	%	Uniform	-12.5	12.5
$\Gamma_{m,6}$	ΔD_1 steel profile diameter	%	Uniform	-1	1
$\Gamma_{m,7}$, $\Gamma_{p,5}$	ΔD_2 steel profile diameter	%	Uniform	-1	1
$\Gamma_{m,8}$	ΔW truck-axle weight	kN	Uniform	-1	1

or asymmetrically with respect to bridge traffic lanes. Potential sensor locations and types are shown in
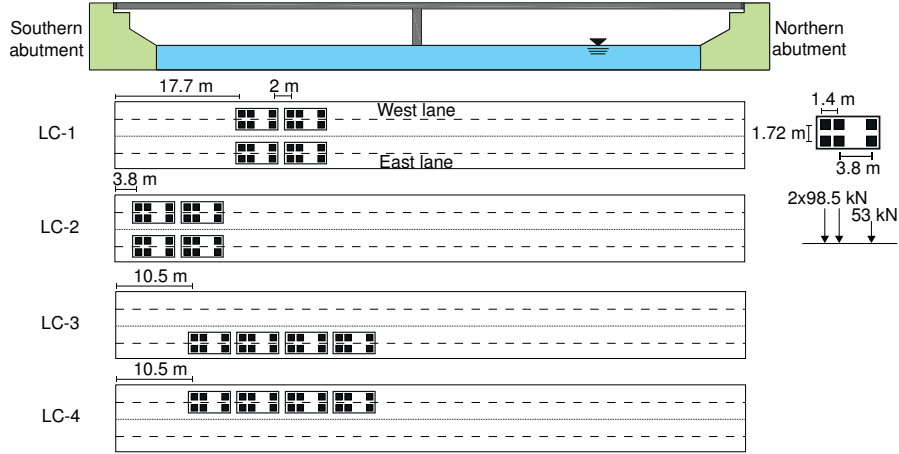

Figure 8: Potential load-test configurations for measurement-system design.

Figure 9. Overall 30 sensor types and locations are possible, including four displacement sensors, nine inclinometers and 17 strain gages. Along with the four load-test configurations, 120 measurements are possible. Displacement gages are positioned to measure the displacement of the southern and northern expansion joint. Inclinometers are located on the bottom chord of east-side truss. Strain gages are located in the middle of the truss braces on the east and west side since it has been noted by previous studies that parameter values were more sensitive at those locations [21].

The cost of a connection reparation is assumed to be $c_r = 15\,000\,\$$ and the discount rate is taken to be
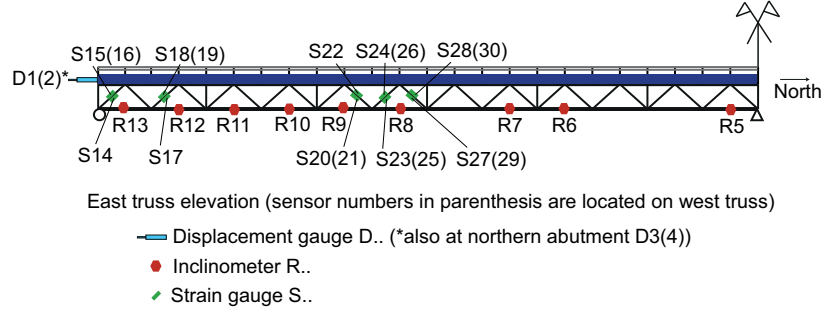
Figure 9: Potential sensor locations and types for measurement-system design.

$i = 1\%$ which represents a good approximation of swiss interest rates including the effect of inflation. It is assumed that displacement sensors, inclinometers, strain gages cost respectively $\$200$, $\$600$ and $\$200$. Also, each truck is expected to have a fix cost $\$400$ and then $\$200$ per hour of use. Each load case lasts two hours.

The initial population of models is generated with $3\,125$ instances based on the uniform sampling of the initial ranges displayed in Table 1. Parametrized sources of modeling uncertainties are displayed in Table 2 and are estimated using Monte Carlo simulations for the potential load cases and measurement locations. Note that they already include correlation estimates since they are evaluated through the FE model.

Other modeling and measurement uncertainties are presented in Table 3 for each sensor type including the qualitative estimate of correlations based on Figure 2. Uncertainties and correlations are estimated

Table 3: Other sources of uncertainty involved in the measurement-system design for each sensor type and qualitative correlation values assigned between sensor types for the Aarwangen Bridge.

	Displacement [mm]		Rotation [μrad]		Strain [$\mu\epsilon$]		Correlation
Uncertainty source	Min	Max	Min	Max	Min	Max	Qualitative
Model simplifications [%]	0	2	0	2	0	5	High+
Mesh refinement [%]	-2	0	-2	0	-2	0	High+
Additional uncertainty [%]	-1	1	-1	1	-1	1	Moderate+
	Mean	SD	Mean	SD	Mean	SD	
Sensor resolution [absolute unit]	0	0.1	0	2	0	1	Low+
Cable losses [%]	0	0	0	0	0	1	Low+
Repeatability [%]	0	1.5	0	1.5	0	1.5	High+
Truck position [%]	0	1.5	0	1.5	0	1.5	Moderate+

using engineering judgment and field heuristics. Model simplifications, mesh refinement and measurement repeatability are sources of uncertainty that may have high interaction between measurement types and locations so that a high correlation is assigned. Conversely, sensor resolution and cables losses induce uncertainties that are almost independent and therefore, a low correlation is assigned. The other sources

may have a moderate degree of correlation. Note that all correlation values are assumed positive.

The greedy algorithm is launched with the initial sets of all load-case and sensor configurations. For each set of simulated measurements, model instances are falsified using Eq. (5) with $\phi = 0.95$. Depending on the number of measurements, coverage regions are adjusted according to ϕ^{1/n_y}, such that more measurements lead to wider coverage regions. The remaining fatigue life is then computed using the obtained candidate-model set using the constant nominal stress-range approach (Section 2.2.1) and using identical accommodation of modeling uncertainties. The process then continues with expected-utility maximization and sensor removal as explained in Section 2.3.2 until a single load case and sensor location are left.

3.1. Aarwangen Bridge sensor placement

Figure 10 presents the results of the measurement-system design for the four critical connections of the Aarwangen Bridge. This figure shows the overall number of measurements including the number of load configurations used for data interpretation in relation with the maximum expected utility. Note that the expected utility is represented relatively to the value computed without monitoring actions in order to have zero utility when no measurement is taken. It is observed that each measurement system leads to an expected utility that is below the utility without monitoring. This means that any measurement system is unprofitable since the optimum expected utility is obtained when no measurement is taken. The linear
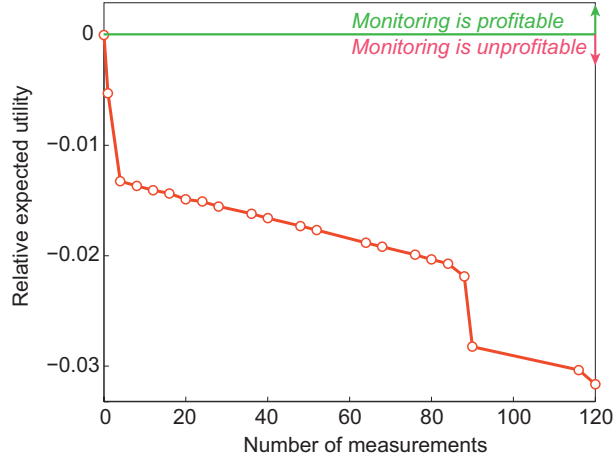

Figure 10: Expected utility in relation with the number of measurements for the Aarwangen Bridge. The almost linear behavior of the solutions are insensitive to change in remaining-fatigue-life predictions between sensor configuration and thus, are dominated by the load test costs. The monotonically decreasing relative expected utility with respect to costs indicate that any monitoring intervention is unprofitable.

trend of the curve reveals a domination of the monitoring cost c_m over the reparation costs. Indeed, the fatigue reserve capacity of these connections are around 500 years meaning that the actualization of the reparation cost leads to very low values. This is due to the division by $(1 + 0.01)^{500}$ in Eq. (13), which leads to the an actualized reparation cost of approximately US\$ 400 when summed for the four connections.

This is understandable that an outcome in 500 years has a very low value presently. Thus, since monitoring costs vary between US\$ 3 400 and 17 600, the effect of actualized reparation costs is low such that monitoring interventions would be unprofitable for any measurement system. In this curve, the monitoring cost c_m is mainly related with $\ln(const - c_m)$ leading a logarithmic-curve segments that seem linear.

These results demonstrate that monitoring interventions are not always necessary and profitable. This methodology is thus able to detect monitoring of infrastructure that is unjustified according to utility as defined in this paper.

3.2. Modified Aarwangen Bridge sensor placement

In order to illustrate the potential of this approach when monitoring actions are profitable, an example is simulated from the Aarwangen Bridge model predictions. The amplitude of stress-ranges are multiplied by three for all initial model instances. The remaining-fatigue-life predictions are thus reduced. This case has higher actualization values of the reparation costs and is more representative of situations common to aging infrastructure. Also, the number of critical connections to evaluate is increased to 40 by replication of available stress-ranges.

Equivalent assumptions are made regarding c_r, i and the costs of trucks and sensors. Figure 11 presents the results of the measurement-system design for this illustrative example. It is shown that monitoring may

Figure 11: Expected utility in relation with load test costs for an illustrative example based on the Aarwangen Bridge. An optimum measurement system is found for six measurements. For a lesser number of measurements than this optimum, measurements are useful and profitable. Adding more measurements would reduce the efficiency of monitoring interventions and data interpretation even if the monitoring is profitable. For more than 30 measurements, monitoring becomes unprofitable.

be useful and profitable. Indeed, for a number of measurements lesser than 30, the expected utility is larger

than the utility without monitoring such that most measurement systems are in the profitable region. For a number of measurements greater than 30, monitoring interventions and data interpretation are unprofitable. In addition, the methodology is able to identify an optimum measurement system for six measurements. The measurement system that leads to the best expected utility is obtained using two displacement sensors (D1 and D2) and one strain gage (S24) under LC-1 and LC-2.

In addition, it is shown that, beyond this optimum, adding more measurements will lead to over-instrumentation as represented by the performance decrease. Indeed, for higher investments in monitoring, the expected utility of such measurement systems becomes equivalent to the situation of lower monitoring investment. The optimum means that a present investment of $5\,400\,\$$ for a monitoring system of three sensors and two load cases will lead to profitable reparation in the future since the money saved by avoiding an early reparation can be invested with return of interest. Table 4 presents the optimal measurement configurations obtained in Figure 11.

Table 4: Best measurement systems with respect to cost. Symbols ◇ indicate selection of sensor and load case.

Load-test configurations (column headers below give the "# of measurements"; the last row gives "LC cost (10^3 US\$)").

Sensors & load-cases	1	2	3	4	6	20	22	22	30	40	42	42	46	60	69	81	84	112	116	120
D1	◇	◇	◇	◇	◇	◇	◇	◇	◇	◇	◇	◇	◇	◇	◇	◇	◇	◇	◇	◇
D2		◇	◇	◇	◇	◇	◇	◇	◇	◇	◇	◇	◇	◇	◇	◇	◇	◇	◇	◇
D3			◇						◇	◇	◇	◇	◇	◇	◇	◇	◇	◇	◇	◇
D4														◇		◇	◇	◇	◇	◇
R5															◇	◇	◇	◇	◇	◇
R6										◇	◇	◇	◇	◇	◇	◇	◇	◇	◇	◇
R7										◇	◇	◇	◇	◇	◇	◇	◇	◇	◇	◇
R8									◇		◇	◇	◇	◇	◇	◇	◇	◇	◇	◇
R9											◇	◇	◇	◇	◇	◇	◇	◇	◇	◇
R10																◇	◇	◇	◇	◇
R11														◇	◇	◇	◇	◇	◇	◇
R12								◇		◇	◇	◇	◇	◇	◇	◇	◇	◇	◇	◇
R13								◇	◇	◇	◇	◇	◇	◇	◇	◇	◇	◇	◇	◇
S14										◇	◇	◇	◇	◇	◇	◇	◇	◇	◇	◇
S15						◇			◇	◇	◇	◇	◇	◇	◇	◇	◇	◇	◇	◇
S16						◇			◇	◇	◇	◇	◇	◇	◇	◇	◇	◇	◇	◇
S17									◇	◇	◇	◇	◇	◇	◇	◇	◇	◇	◇	◇
S18										◇	◇	◇	◇	◇	◇	◇	◇	◇	◇	◇
S19										◇	◇	◇	◇	◇	◇	◇	◇	◇	◇	◇
S20						◇	◇	◇	◇	◇	◇	◇	◇	◇	◇	◇	◇	◇	◇	◇
S21						◇	◇	◇	◇	◇	◇	◇	◇	◇	◇	◇	◇	◇	◇	◇
S22						◇	◇	◇	◇	◇	◇	◇	◇	◇	◇	◇	◇	◇	◇	◇
S23											◇	◇	◇	◇	◇	◇	◇	◇	◇	◇
S24					◇	◇	◇	◇	◇	◇	◇	◇	◇	◇	◇	◇	◇	◇	◇	◇
S25														◇	◇	◇	◇	◇	◇	◇
S26						◇	◇	◇	◇	◇	◇	◇	◇	◇	◇	◇	◇	◇	◇	◇
S27						◇	◇	◇	◇	◇	◇	◇	◇	◇	◇	◇	◇	◇	◇	◇
S28											◇	◇	◇	◇	◇	◇	◇	◇	◇	◇
S29			◇			◇	◇	◇	◇	◇	◇	◇	◇	◇	◇	◇	◇	◇	◇	◇
S30						◇	◇	◇	◇	◇	◇	◇	◇	◇	◇	◇	◇	◇	◇	◇
LC-1	◇	◇	◇	◇	◇	◇	◇	◇	◇	◇	◇	◇	◇	◇	◇	◇	◇	◇	◇	◇
LC-2		◇	◇	◇	◇	◇	◇	◇	◇	◇	◇	◇	◇	◇	◇	◇	◇	◇	◇	◇
LC-3												◇	◇	◇	◇	◇	◇	◇	◇	◇
LC-4									◇							◇	◇	◇	◇	◇
# of measurements	1	2	3	4	6	20	22	22	30	40	42	42	46	60	69	81	84	112	116	120
LC cost (10^3 US\$)	3.4	3.6	3.8	5.2	5.4	6.8	7.0	7.4	8.4	9.6	9.8	10.2	11.0	11.2	12.6	15.0	15.6	17.2	17.4	17.6

4. Discussion

This utility-based measurement-system-design strategy involves the assumption of a constant discount rate during the period of fatigue damage accumulation that may theoretically last for centuries. However, although the assumption of having the same discount rate 100 years from now is weak and may bias the expected utility values, the optimal measurement system is insensitive to the choice of the discount rate. Indeed, since the present value is a monotonic function, an increase in discount rate reduces the actualized reparation cost and thus increases the expected utility of all potential measurement systems such that the relative utility of each measurement system is preserved as it would be with a lower discount rate. This argument has been verified with the example of the Aarwangen Bridge for discount rates of 2% and 5% leading to the same optimal measurement system as the results with $i = 1\%$. The difference resides only in the absolute values of expected utility and in a variation in the extent of the profitable monitoring region.

The same observation can be made with the choice of the utility function. However, the logarithmic function, apart of the advantage of describing a risk-averse behavior of the decision maker, allows for assigning a larger expected utility to PDFs of total cost Z'' that have less uncertainty for equivalent expected total cost value.

Compared with other approaches presented in Section 1, this methodology provides a direct evaluation of the utility of measurement systems. Although entropy-based techniques are appropriate for the determination of the most informative measurement systems, the estimation of the expected utility based on the cost of improving remaining-fatigue-life predictions is efficient to support engineering decision-making in a more comprehensive way. Note that this methodology may be adapted to other types of time-dependent prognoses. Indeed, the calculation of the reparation costs would only require to be adapted to the prognosis type.

5. Conclusions

This methodology based on the maximization of the expected utility allows evaluation of expected improvements in critical limit states such as fatigue reserve capacity in terms of future infrastructure reparation costs. Conclusions are as follows:

- The utility-based measurement-system-design methodology proposed is able to quantify the optimal expected utility of monitoring actions using remaining-fatigue-life estimations and cost considerations.

- This strategy evaluates whether or not monitoring actions are profitable and when measurement-system performance becomes reduced by over-instrumentation.

- By evaluating the utility of monitoring actions at the prognosis stage, this sensor-placement methodology provides direct guidance for decisions related to the process of structural health management

20

while current approaches that are often limited to the diagnosis-stage optimization may not provide such support.

Acknowledgements

References

[1] AASHTO, 2007. LRFD Bridge Design Specifications. 4th Edition, American Association of State Highway and Transportation Officials, Washington, DC.

[2] Bernoulli, D., 1954. Exposition of a new theory on the measurement of risk. Econometrica: Journal of the Econometric Society, 23–36.

[3] Brito, A., de Almeida, A., 2009. Multi-attribute risk assessment for risk ranking of natural gas pipelines. Reliability Engineering & System Safety 94 (2), 187–198.

[4] EN1993-1-9, 2005. Eurocode 3 - Design of steel structrures - Part 1-9: Fatigue. European committee for standardization.

[5] Ferreira, R., de Almeida, A., Cavalcante, C., 2009. A multi-criteria decision model to determine inspection intervals of condition monitoring based on delay time analysis. Reliability Engineering & System Safety 94 (5), 905–912.

[6] Georgy, M., Chang, L.-M., Zhang, L., 2005. Utility-function model for engineering performance assessment. Journal of Civil Engineering and Management 131 (5), 558–568.

[7] Goulet, J.-A., Smith, I., 2013. Performance-driven measurement system design for structural identification. Journal of Computing in Civil Engineering 27 (4), 427–436.

[8] Goulet, J.-A., Smith, I., 2013. Predicting the usefulness of monitoring for identifying the behavior of structures. Journal of Structural Engineering 139 (10), 1716–1727.

[9] Goulet, J.-A., Smith, I., 2013. Structural identification with systematic errors and unknown uncertainty dependencies. Computers & Structures 128, 251–258.

[10] Heredia-Zavoni, E., Montes-Iturrizaga, R., Esteva, L., 1999. Optimal instrumentation of structures on flexible base for system identification. Earthquake engineering & structural dynamics 28 (12), 1471–1482.

[11] Kang, F., Li, J.-J., Xu, Q., 2008. Virus coevolution partheno-genetic algorithms for optimal sensor placement. Advanced Engineering Informatics 22 (3), 362–370.

[12] Kripakaran, P., Smith, I., 2009. Configuring and enhancing measurement systems for damage identification. Advanced Engineering Informatics 23 (4), 424–432.

[13] Machina, M., 1987. Decision-making in the presence of risk. Science 236 (4801), 537–543.

[14] North, D., 1968. A tutorial introduction to decision theory. IEEE Transactions on Systems Science and Cybernetics 4 (3), 200–210.

[15] Papadimitriou, C., 2004. Optimal sensor placement methodology for parametric identification of structural systems. Journal of Sound and Vibration 278 (4), 923–947.

[16] Papadimitriou, C., 2005. Pareto optimal sensor locations for structural identification. Computer Methods in Applied Mechanics and Engineering 194 (12), 1655–1673.

[17] Papadimitriou, C., Beck, J., Au, S.-K., 2000. Entropy-based optimal sensor location for structural model updating. Journal of Vibration and Control 6 (5), 781–800.

[18] Papadimitriou, C., Lombaert, G., 2012. The effect of prediction error correlation on optimal sensor placement in structural dynamics. Mechanical Systems and Signal Processing 28, 105–127.

[19] Papadopoulou, M., Raphael, B., Smith, I., Sekhar, C., 2014. Hierarchical sensor placement using joint entropy and the effect of modeling error. Entropy 16 (9), 5078–5101.

[20] Pasquier, R., D'Angelo, L., Goulet, J.-A., Acevedo, C., Nussbaumer, A., Smith, I., 2015. Measurement, data interpretation, and uncertainty propagation for fatigue assessments of structures. Journal of Bridge Engineering in press.

[21] Pasquier, R., Goulet, J.-A., Acevedo, C., Smith, I., 2014. Improving fatigue evaluations of structures using in-service behavior measurement data. Journal of Bridge Engineering 19 (11), 04014045.

[22] Pozzi, M., Der Kiureghian, A., 2011. Assessing the value of information for long-term structural health monitoring. In: SPIE Smart Structures and Materials+ Nondestructive Evaluation and Health Monitoring. International Society for Optics and Photonics, pp. 79842W–79842W.

[23] Pozzi, M., Zonta, D., Wang, W., Chen, G., 2010. A framework for evaluating the impact of structural health monitoring on bridge management. In: Proc. 5th Int. Conf. Bridge Maintenance, Safety Manage. p. 161.

[24] Qureshi, Z., Ng, T., Goodwin, G., 1980. Optimum experimental design for identification of distributed parameter systems. International Journal of Control 31 (1), 21–29.

[25] Robert-Nicoud, Y., Raphael, B., Smith, I., 2005. Configuration of measurement systems using Shannon's entropy function. Computers & structures 83 (8), 599–612.

[26] SIA263 Code, 2003. Norme SIA 263 : Steel structures. SIA Zurich.

[27] Stephan, C., 2012. Sensor placement for modal identification. Mechanical Systems and Signal Processing 27, 461–470.

[28] Worden, K., Burrows, A., 2001. Optimal sensor placement for fault detection. Engineering Structures 23 (8), 885–901.

[29] Yi, T.-H., Li, H.-N., Gu, M., 2011. Optimal sensor placement for structural health monitoring based on multiple optimization strategies. The Structural Design of Tall and Special Buildings 20 (7), 881–900.

[30] Yi, T.-H., Li, H.-N., Zhang, X.-D., 2015. Health monitoring sensor placement optimization for Canton Tower using immune monkey algorithm. Structural Control and Health Monitoring 22 (1), 123–138.

[31] Zhao, X.-L., Herion, S., Packer, J., Puthli, R., Sedlacek, G., Wardenier, J., Weynand, K., van Wingerde, A., Yeomans, N., 2002. Design guide for circular and rectangular hollow section welded joints under fatigue loading. TÜV-Verlag GmbH.

[32] Zonta, D., Glisic, B., Adriaenssens, S., 2014. Value of information: impact of monitoring on decision-making. Structural Control and Health Monitoring 21 (7), 1043–1056.